

Nanoparticles and nanostructures formed by laser: what can we learn from the modeling?

Tatiana E. Itina,^{1*} Nawfel Bouflous,¹ Jörg Hermann,² and Philippe Delaporte²

¹Laboratoire Hubert Curien, CNRS UMR 5516/Université de Lyon, Saint Etienne, France

²Laboratoire Lasers, Plasmas et Procédés Photoniques, CNRS UMR 6182, Marseille, France

ABSTRACT

The processes involved in nanoparticle and nanostructure formation by laser are analyzed. Relative contributions of several mechanisms involved are compared. First, we consider the formation of “primary” particles and discuss the difference between femtosecond and nanosecond regimes. Then, “secondary” particle/aggregate formation is discussed. In particular, attention is focused on (i) direct cluster ejection from a target under rapid laser interaction; (ii) condensation/evaporation; (iii) fragmentation/aggregation processes during cluster diffusion; (iv) diffusion, aggregation, and/or coalescence. In addition, routes of control over particle size distribution are proposed. Possibility of formation of colloidal nanoparticles with very narrow size distribution is proven numerically. The role of such parameters as ablation yield, laser wavelength and laser fluence, and surface tension are examined. Finally, controlled nanoparticle self-assembly is discussed as a potential technique for future development of nanomaterials.

Keywords: Laser, primary nanoparticles, aggregates, modeling, ablation, colloids, shape of size distribution, self-assembly, nanomaterials.

1. INTRODUCTION

Laser-produced nanoparticles (NPs) have found many applications in medicine, bio-photonics, in the development of sensors, new materials and solar cells. Laser interactions provide a possibility of chemically clean synthesis, which is difficult to achieve under more conventional NP production conditions. Moreover, a careful optimization of the experimental conditions can allow a control over size distributions of the produced nanoclusters. Therefore, many studies were focused on the investigation the laser nanofabrication.^{1,2,3,4,5,6,7,8,9,10,11} In particular, many experiments were performed demonstrating NP formation in vacuum, in the presence of a gas or a liquid. Nevertheless, it is still difficult to control the properties of the produced particles. We believe that numerical calculations can help to explain experimental results and to better understand the mechanisms involved.

Despite rapid development in laser physics, one of the fundamental questions still concerns the definition of proper ablation mechanisms and the processes leading to the NP formation. Apparently, the progress in laser systems implies several important changes in these mechanisms, which depend on both laser parameters and material properties. Among the more studied ablation mechanisms there are thermal, photochemical and photomechanical ablation processes. Frequently, however, the mechanisms are mixed, so that the existing analytical equations are hardly applicable. In this case, numerical simulation is needed to better understand and to optimize the ablation process.^{12,13,14} So far, thermal models are commonly used to describe nanosecond (and longer) laser ablation.^{15,16} In these models, the laser-irradiated material experiences heating, melting, boiling and evaporation. Thermal effect plays therefore a major role, particularly

* E-mail: tatiana.itina@univ-st-etienne.fr; phone 33 477 91 5829; fax 33 477 91 5781;

in the case of metals with high thermal conductivity. In this case, the ablation flux can be described by a Hertz-Knudsen equation. The interaction of femtosecond pulses even with metals implies, however, a change in the ablation mechanism due to not only the absence of equilibrium between electrons and lattice-ions during the pulse, but also because the heating is too fast. The Hertz-Knudsen equation is inapplicable in this case and a numerical study is for the careful optimization of the laser processing of metals.

Recently, many experimental and theoretical investigations of the mechanism of femtosecond (< 100 fs) ablation have been performed.^{17,18,19,20} Evidently, the interest in femtosecond lasers was caused by numerous exciting laser applications listed above. Among the main advantages of these short pulses is the possibility of laser treatment of any materials, even these that were considered to be transparent, in a possibility of control over electronic excitations, and in the minimization of non-desirable thermal effects. However, the mechanisms of these interactions are often rather different from that of longer pulses, and many difficulties first arouse in the corresponding numerical modeling. The main point that makes ultra-short interactions difficult to model, is that the pulse duration is shorter than the electron-phonon/ion relaxation time $t_{ei} \sim 1-10$ ps. As a result of strong difference between the electron and ion mass, the mean electron energy rises much faster and higher than that of ion subsystem. The terms “electron and ion temperatures”, however, require equilibrium in each sub-system that also may take longer time to establish. If these terms can be applied, electron temperature is much larger than ion temperature during the interaction. The knowledge about the required equation of state (EOS) is also very limited. In addition, metastable matter states, such as superheated liquid one, seem to play a role. All these points limit the information about model parameters and make computer simulation rather difficult.

In studies of picosecond and femtosecond interactions, new ablation mechanisms have been proposed both for metals and semiconductor materials.^{17,18,19,21,22,23,24,25,26,27,28,29} To calculate material motion (and not only its temperatures), three numerical approaches were used, such as

-*Atomistic approach*, based on such methods as molecular dynamics (MD)^{21,30,31,32} and Direct Monte Carlo Simulation (DSMC).^{33,34,35} Typical calculation results provide detailed information about atomic positions, velocities, kinetic and potential energy;

-*Macroscopic approach based hydrodynamic models*.^{14,36,37} These models allow the investigations of the role of the laser-induced pressure gradient, which is particularly important for ultra-short laser pulses. The models are based on a one fluid two-temperature approximation and a set of additional models (equation of state) that determines thermal properties of the target;

-*Multi-scale approach* based on the combination of two approaches cited above was developed by several groups and was shown to be particularly suitable for laser applications.

The ejection of liquid and/or solid particulates has been studied for metals,^{38,39,40} semiconductors,^{41,42,43,44} dielectrics,^{45,46} and organic materials.⁴⁷ The parameters of the ejected particles are found to have a strong dependence on the laser irradiation conditions and the background gas pressure. A number of scenarios of cluster formation in laser ablation have been discussed in the literature. In many cases, observation of small clusters is attributed to the collision-induced condensation in the dense regions of the ejected plume.^{44,46,48,49} Some evidences of the direct ejection of nanoparticles by ultra-short laser pulses were also obtained.

Herein, we compare the relative contribution of the processes involved in the NP's production by laser ablation. In addition, the origins of the shape of the cluster size distribution are presented. First, “primary” particles are considered. Then, “secondary” particle/aggregate formation is discussed. Such processes as direct cluster ejection from a target under rapid laser interaction; condensation/evaporation; fragmentation/aggregation processes during cluster diffusion, diffusion, aggregation, and/or coalescence are examined. Future trends in the field of laser-assisted nano-fabrication are discussed.

2. EVIDENCES OF NANOPARTICLE FORMATION BY LASER ABLATION

To check the formation of NPs by short and ultra-short laser pulses, a series of experiments was performed.^{50,51,52} These experiments demonstrated that

-the observed NPs were deposited on a distant target; the shape of their typical size distribution was fitted by a decreasing function [Figure 1(a,b)];

-NPs were found in the laser ablated plume. In particular, when femtosecond laser was used, two distinct components were observed in the plume: the fast one composed of atoms and ions and the slow one composed of laser NPs [Figure 1(c)].

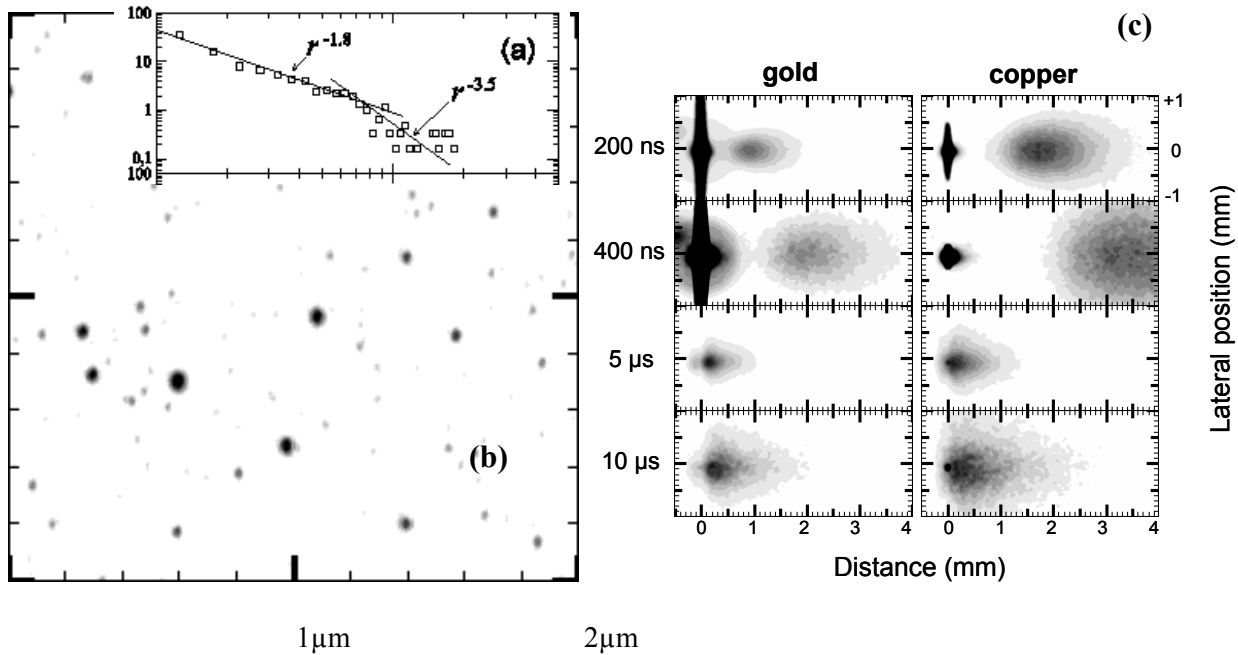


Figure 1. (a) - Size distribution of laser-produced nanoparticles; (b) -AFM image (2 μm x 2 μm) of gold nanoparticles deposited on a mica substrate by 4500 laser pulses of 800nm wavelength with laser fluence of 0.9 Jcm⁻²; (c) - Plume images recorded during ablation of gold and copper for several times and a laser fluence of 4 J cm⁻² the target is on the left side of the figure.

Furthermore, previously the cumulative number density $f(A)$ of NP's (from infinity to A) as measured by the AFM was found to fit well by the following equation⁵³

$$f(A)[particles / \mu m^2] = \alpha_1 \exp\left(-\frac{A}{\mu_1}\right) + \alpha_2 \exp\left(-\frac{A}{\mu_2}\right), \quad (1)$$

where A is the area of the measured NP in units of nm² and other parameters, α_1 , μ_1 , α_2 , and μ_2 are fitting constants.

Interestingly, in the presence of a background gas or a liquid, the shape of NP's size distribution was different and more often could be fitted by a log-normal function. The position of the maximum, or a most probable size of NPs, as well as the width of the distribution (dispersion) depend strongly on laser parameters, on target material properties and on the properties of a background medium. Interestingly, very small NP with rather narrow size distribution could be produced in liquids with the addition of surfactant molecules. The origin of such shape of NP's size distribution will be discussed in what follows.

3. NUMERICAL ANALYSIS OF “PRIMARY” NANOPARTICLE FORMATION BY SHORT LASER ABLATION

In this section we consider the basic mechanisms of “primary” NP formation by short-pulsed laser interactions. The term “primary” particles designates here particles that are either directly ejected from the laser-irradiated target (short and ultra-short laser pulses), or particles that are formed by nucleation in laser-generated plume.

3.1 Direct laser-induced ejection of nanoparticles

For a rather long time, laser was considered as a source of heat, and laser ablation process was associated as a set of phase transitions, such as melting and evaporation. Long before the appearance of short and ultra-short laser pulses, only direct ejection of droplets from the laser-irradiated target was attributed to the effect of background pressure on laser-melted zone. Based on such a concept, NPs could be formed only by nucleation and condensation in the evaporated vapor. Thus, rather high ablation yield and/or very fast vapor plume expansion were crucial for vapor supersaturation and nucleation. Therefore, nucleation process, requiring the formation of surface energy of particles, was considered only in several studies. These studies have demonstrated that NP formation could be enhanced when long laser pulses were used in vacuum, when a series of laser pulses was used, and/or when ablation took place in the presence of a background environment.

Recently, laser systems with very short and intense pulses have opened a new vision of laser-matter interaction. These interactions are characterized by the absence of equilibrium between electron and lattice/ions subsystems allowing the reduction of thermally affected zones. Secondly, such short laser pulses create very strong shock waves propagating inside the target and leading to fast explosion-like target decomposition driven by the rarefaction wave. Finally, it was shown that target material can be heated near or even above the critical point, so that the target material enters into both metastable and unstable regions of the corresponding phase diagram (Figure 2a).

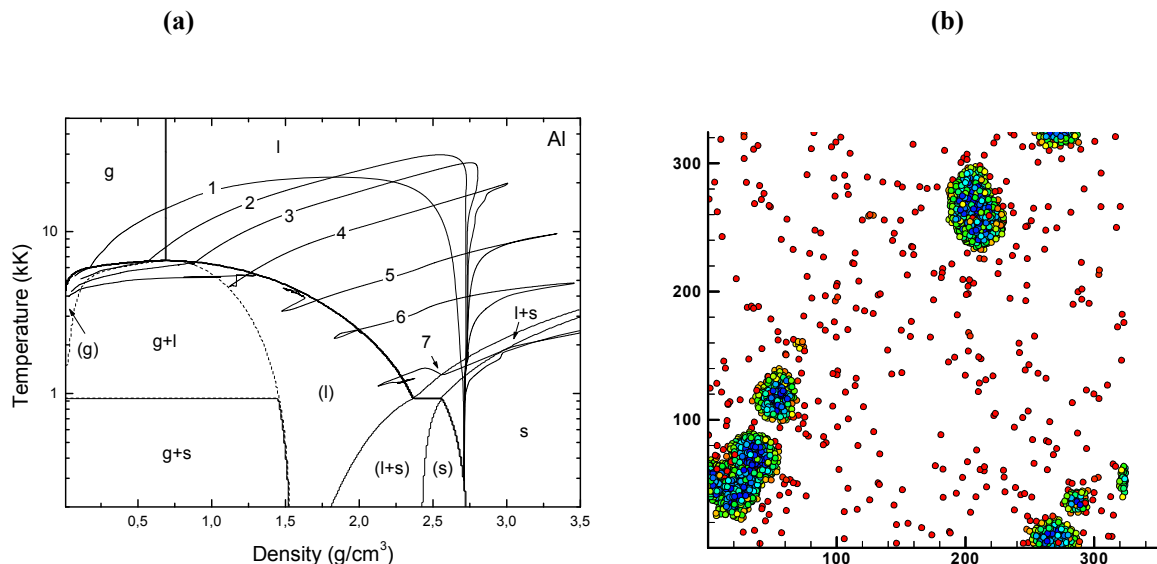


Figure 2. (Color online) (a) –Phase diagram and trajectories originated from different target layers below the irradiated surface (here, 5, 15, 20, 30, 50, 80, 130 nm). Here, “s” means solid, “l” means liquid, “g” means gas, (l) means superheated liquid, (g) means supercooled gas, etc. Laser parameters are the following: pulse width $\tau = 100$ fs, wavelength $\lambda = 800$ nm, and fluence $F = 5.0$ J/cm². (b) –MD simulation of rapid target fragmentation leading to particle formation, numbers on the axes are in angstroms.

In such regions, laser-irradiated target is directly decomposed into a mixture of gas and liquid particles. Models based on thermal equilibrium cannot describe these processes and new non-equilibrium approaches are required. Therefore, the appropriate models were developed based on either molecular dynamics simulation or on hydrodynamic modeling. Calculations performed with such models for ultra-short laser ablation in vacuum confirmed the effect of target decomposition into a mixture of gas and small particles. Thus, both molecular dynamics and larger-scale numerical hydrodynamics clearly explained the ejection of particles from laser-irradiated targets when laser pulse duration is on the order of 100 ps or shorter. The corresponding thermodynamic analysis was performed for different materials ranging from molecular solids to semiconductors and metals. These theoretical results agree with a number of experiments. This result does not exclude the possibility of nucleation and condensation, in particular if ablation takes place in ambient gas, air or liquid.

3.2 The role of nucleation in NP's formation

Nucleation is a non-equilibrium process bringing a supersaturated system to a new equilibrium state. Nucleation can be observed when the formation of a new phase is energetically profitable.^{54,55,56,57,58}

When homogeneous nucleation takes place in a vapor, then it refers to the formation of small stable clusters of vapor molecules, or nuclei (small liquid particles) in a supersaturated vapor. When this process occurs in a liquid solution (as, for instance, in the solution of gold atoms in water), this process means the formation of small gold clusters or particles in the solution. In both cases, the process requires supersaturation of gas or of a solution. Let us denote the saturation parameter S that denotes the degree of supersaturation (the system is supersaturated if $S > 1$, or when pressure exceeds the one of the saturated system, Figure 3).

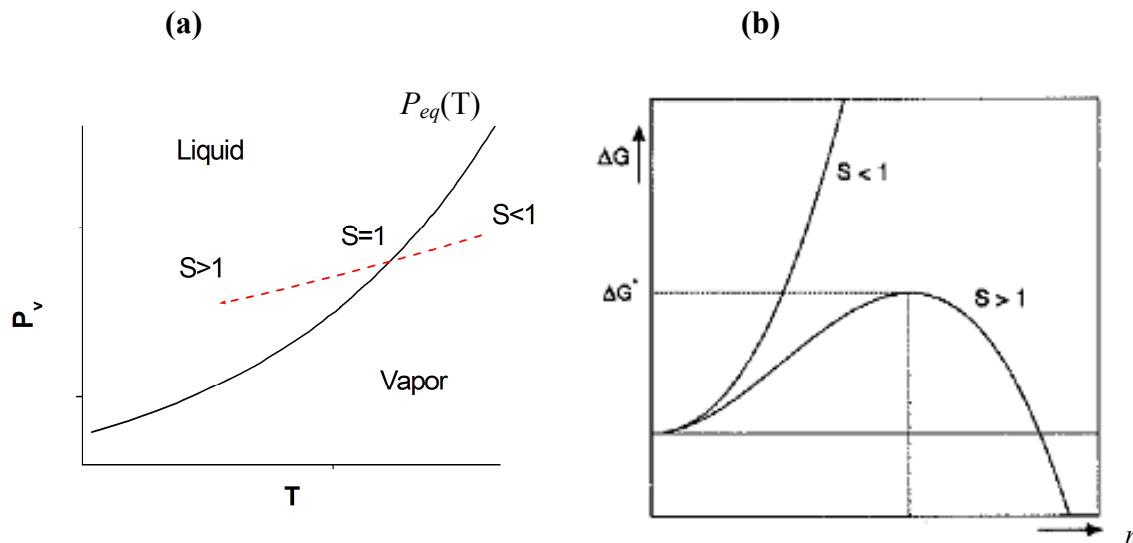


Figure 3. (a) – Saturation curve $P_{eq}(T)$ and the degree of supersaturation; (b) – energy barrier for nucleation as a function of the number of monomers n in the cluster.

The nucleation rate is the rate, at which these nuclei are formed. When the parent phase is supersaturated, these clusters are stable and the system can lower its energy by forming the new phase. This decrease of energy is proportional to the volume of the new phase. The formation of the new phase also involves the formation of an interface between the parent phase and the new phase, which increases the total energy in proportion to the area of this interface. Hence, the difference in the energy of a system with and without a cluster of the new phase has a maximum as a function of the cluster size. This maximum forms an energy barrier for the formation of the new stable phase. This energy barrier can be written as

$$\Delta G = -nkT \ln(S) + 4\pi a^2 n^{2/3} \sigma, \quad (2)$$

where n is the number of monomers in the cluster; T is temperature; k is Boltzmann's constant; a is the effective radius of the monomers, σ is surface tension. The height of this energy barrier is called the energy of cluster formation, and it depends on the degree of super-saturation of the system. The clusters of size corresponding to this maximum are called the critical clusters. According to the classical nucleation theory, the number of atoms in the critical nuclei is

$$N_c = \left[\frac{8\pi a^2 \sigma}{3kT \ln(S)} \right]^3, \quad (3)$$

The further is the system away from equilibrium, the lower is the energy barrier, and the smaller is the critical clusters. The probability of obtaining a critical cluster is proportional to the Boltzmann factor with the energy of formation in the exponent

$$J_{nuc} \propto \exp\left[\frac{-\Delta G}{kT} \right]. \quad (4)$$

Previously, it was demonstrated that nucleation and condensation could occur during rapid laser plume expansion in vacuum⁵⁹. In addition, these mechanisms were shown to explain particle formation in a background gas⁶⁰. Because strong super-saturation is required, the conditions for the nucleation and condensation processes can be checked based on the saturated vapor pressure curve $P_{eq}(T)$ given by the equation of state. In a rapidly expanding plume, the above equations are general and correspond to the local vapor parameters.^{59,60} In the case of laser ablation, laser-produced plasma plume rapidly expands either in vacuum or in a background gas/liquid. In this case, the vapor becomes supercooled and the saturation parameter can be calculated as

$$S = \frac{T_{eq} - T}{T_{eq}}, \quad (5)$$

where T_{eq} is the equilibrium temperature at the local pressure that is obtained from the vapor equation of state, and T is the local temperature. For the estimations of the saturated vapor pressure (vapor-liquid equilibrium), Clausius-Clapeyron equation is used

$$P_{eq} = P_0 \exp\left\{ \frac{Q}{k} \left(\frac{1}{T_b} - \frac{1}{T} \right) \right\}, \quad (6)$$

It should be noted that even if clusters are nucleated in the plume, they can either evaporate or grow, depending on four parameters; their initial size, temperature, local plume temperature and density. The corresponding studies show that smaller and hotter clusters will disappear in the plume.^{9,10}

The condensation-evaporation process can be described by the corresponding balance equation

$$\frac{dr}{dt} = \frac{1}{N} (J_{cond} - J_{evap}), \quad (7)$$

$$J_{cond} = \alpha \frac{P(0)}{(2\pi mkT)^{1/2}}, \quad J_{evap} = N \left(\frac{kT_s}{2\pi m} \right)^{1/2} \exp\left\{ -\frac{Q}{kT_s} \right\}, \quad (8)$$

where α is the sticking coefficient, T_s is temperature at cluster surface.

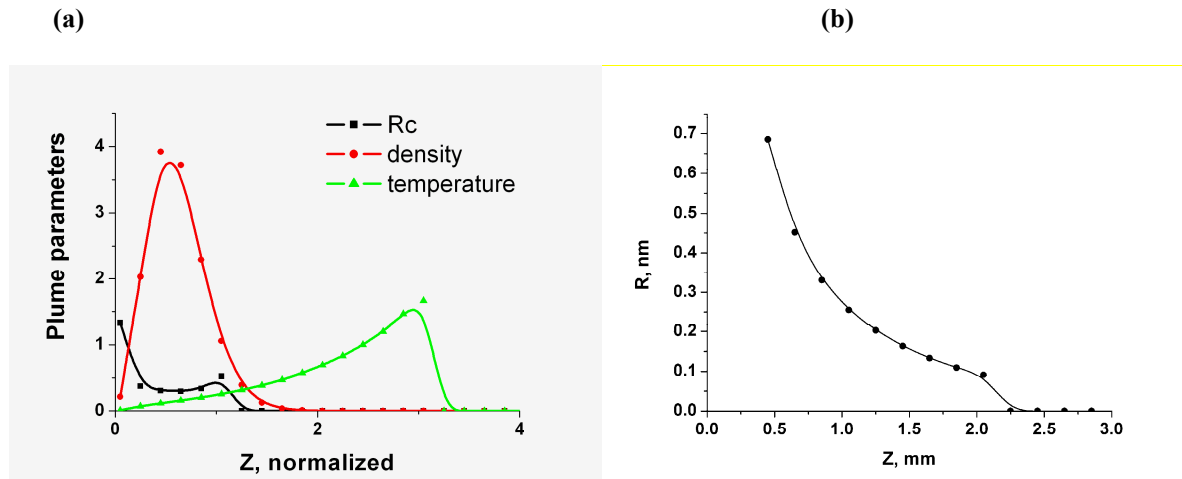


Figure 4. (Color online) (a) –axial distribution of plume density, temperature and the radius of nuclei's radius obtained in a 2D hydrodynamic calculation of laser plume expansion at 40 laser pulse durations. Density and temperature are normalized by their initial values and size by 1 μm . (b) nuclei's radius at a delay of 60 pulse durations. Here, distance is normalized by laser spot radius. Calculations are performed for the ablation of gold with laser pulses of 30 ns, spot radius 1 mm.

By introducing these equations in our two-dimensional model of laser plume expansion we can analyze NPs formation in a laser-generated plume. The calculation results shown in Figure 4 demonstrate that larger NPs are formed at the beginning of the plume expansion in vacuum and mostly at the backside of the plume. This result can be explained by the fact that plume temperature is smaller at this region. For this process to occur, the ablated flux should be high enough providing sufficient loading of the ablated material to insure the supersaturation conditions. These conditions are more easily satisfied for longer laser pulses and larger laser beam spots. This result is in a good agreement with the experimental data.

4. ON THE SHAPE OF NP'S SIZE DISTRIBUTION

It remains now to explain why in some cases NP's distribution could be described by a decreasing function, whereas in other cases lognormal distribution was observed.

4.1 Theoretical analysis of the decreasing size distribution function observed in vacuum

By analyzing the available experimental data, one can note that NP's distribution could be described by a decreasing function when laser ablation took place in vacuum. In this case, secondary particle formation by aggregation or coalescence is negligible. Instead, nanoparticles are either formed by target fragmentation or by nucleation. Interestingly, theoretical analysis of both of these processes leads to a decreasing dependency for NP's size distribution. Fragmentation processes was described in details in Refs. ^{61,62} and we will not repeat these considerations here. In the case of nucleation, the equilibrium density of clusters is given by ⁶³

$$C(n^{cl}) = C_1 \exp\left(-\frac{W(n^{cl}) - W(1)}{kT}\right), \quad (9)$$

Where $W(n^{cl})$ is the energy needed to form the cluster of size n^{cl} . The corresponding dependencies are shown in Figure 5(a). This result can explain experiments.^{51,53} Note that rising part of the green curve $d\mu/kT=2$ is unphysical, so that only decreasing dependency is kept in the case of nucleation.

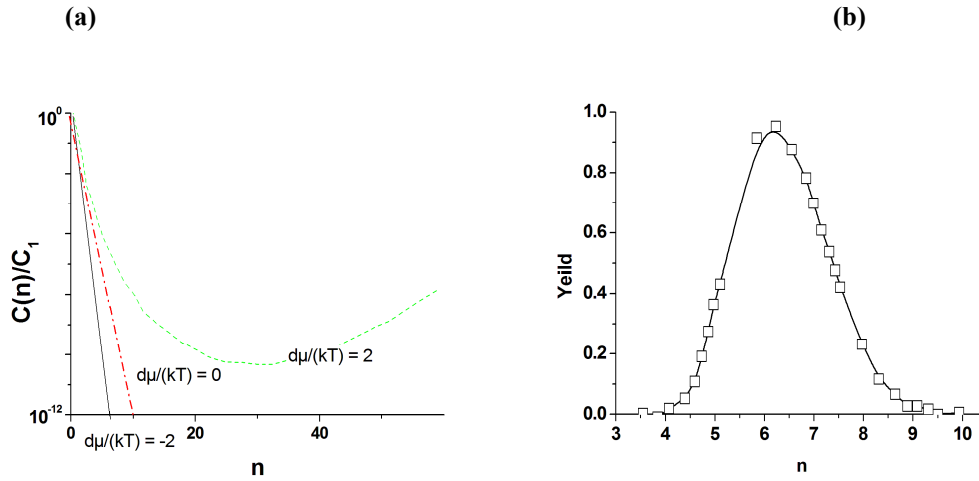


Figure 5. (Color online) (a) Equilibrium size distribution of nucleated particles; here $d\mu$ is the change in the corresponding chemical potential connected to the formation energy W ; (b) -Log-normal size distribution due to secondary particle formation.

4.2. Secondary particle formation: Smoluchowski master equation and lognormal size distribution

Figure 5(b) shows typical NP's size distribution obtained in the presence of a background environment. When laser interaction takes place in the presence of a background gas, or a liquid, initial fast plume expansion is followed by a much longer diffusion and thermalization. At this stage, if density of particles is high enough, coagulation or coalescence processes can take place. These processes are well described by Smoluchowski master equation.⁶⁴

$$\frac{\partial n}{\partial t} = \frac{1}{2} \int_0^v \beta(\tilde{v}, v - \tilde{v}) n(\tilde{v}) n(v - \tilde{v}) d\tilde{v} - \int_0^\infty \beta(v, \tilde{v}) n(\tilde{v}) n(v) d\tilde{v}, \quad (10)$$

with the appropriate kernels β . Interestingly, it was shown⁶⁴ that this equation yields self-preserving log-normal size-distribution of particles (Figure 5b). This very general result can explain the fact that NP's size distributions frequently observed in experiments where background environment promoted particle aggregation/coalescence could be fitted by such functions.

4.3. Control over size distribution: the role of ablation yield and of surface properties

To examine the role of the ablation yield in the size distribution of aggregating NPs, we have solved Smoluckowski equation in a two-step approximation.⁶⁵ The calculation results are shown in Figure 6. One can see (Fig. 6a) that with the increase in the ablation yield, the mean size of NPs grows. This result can be attributed to the enhancement in collision frequency leading to the formation of larger aggregates.

In addition to the ablation yield, NP's surface properties evidently play an important role in NP aggregation. This effect can be seen in Figure 6b that when sticking process is enhanced larger particles are formed. If, on the contrary, NP's surfaces are modified, for instance, by surfactant molecules, much smaller NPs are expected to be obtained with a narrower size distribution.

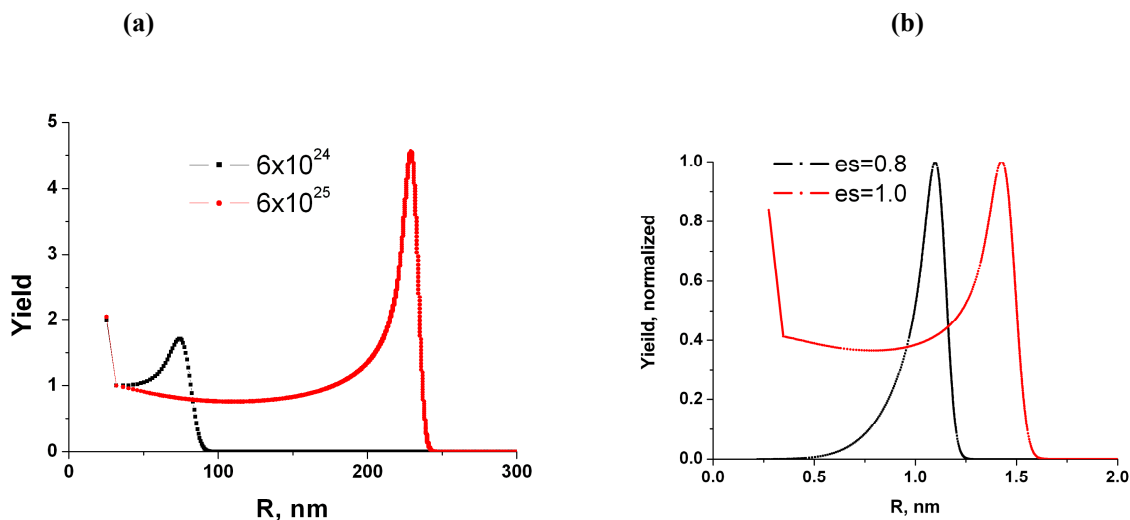


Figure 6. (Color online) (a) –NP’s size distribution calculated for gold solution in water at different solution concentration; (b) –the same distributions calculated for different sticking parameter.

4.4 NP’s deposition, diffusion and coalescence processes on the surface

When NPs are deposited on a surface, their size distribution can be modified by additional processes on the surface. To show their role, a kinetic Monte Carlo method based on Metropolis algorithm was used for gold deposition on carbon substrate. In these calculations, a 2D lattice map (i,j) with periodic boundary conditions is used. The diffusion coefficient $D(T,N)=D(T)N^{-\gamma}$, where N is the number of atoms in the cluster under consideration. Here, γ is a parameter that characterizes the diffusion rate of different clusters and its value depends on the properties of the clusters, as well as the substrate. Here, for simplicity $\gamma=1$. To simulate the coalescence between two clusters, each cluster is assigned a radius r corresponding to its number of atoms $N=4\pi/3r^3\rho_0$. For monomers, the atomic radius of Au atom, r_0 , is used.

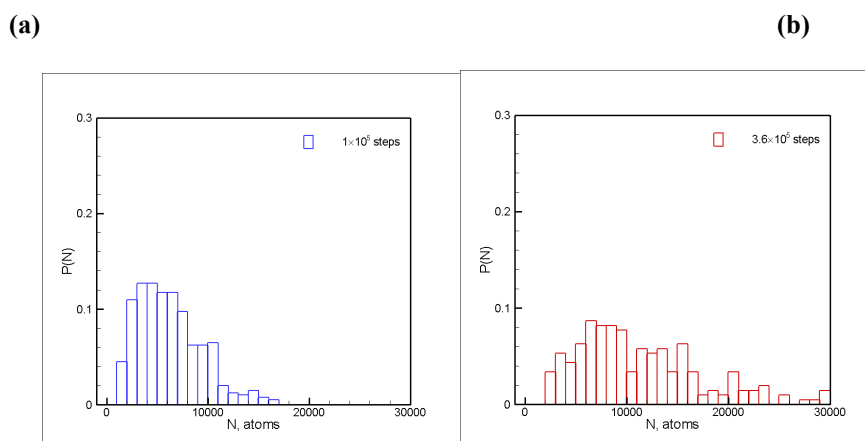


Figure 7 (a) (Color online) Size distribution of the clusters after 105 time steps. (b) - Size distribution of the clusters after 378 time steps. The total number of atoms here is 2.5 millions.

The MC calculation results (Figure 7) clearly demonstrate that the final NP’s size distribution changes with time due to diffusion and coalescence. The final structure and NP’s size distribution depend strongly on the initial distance between them and on the parameter γ defining the diffusion rate.

4.5 NP's size reduction by additional laser irradiation

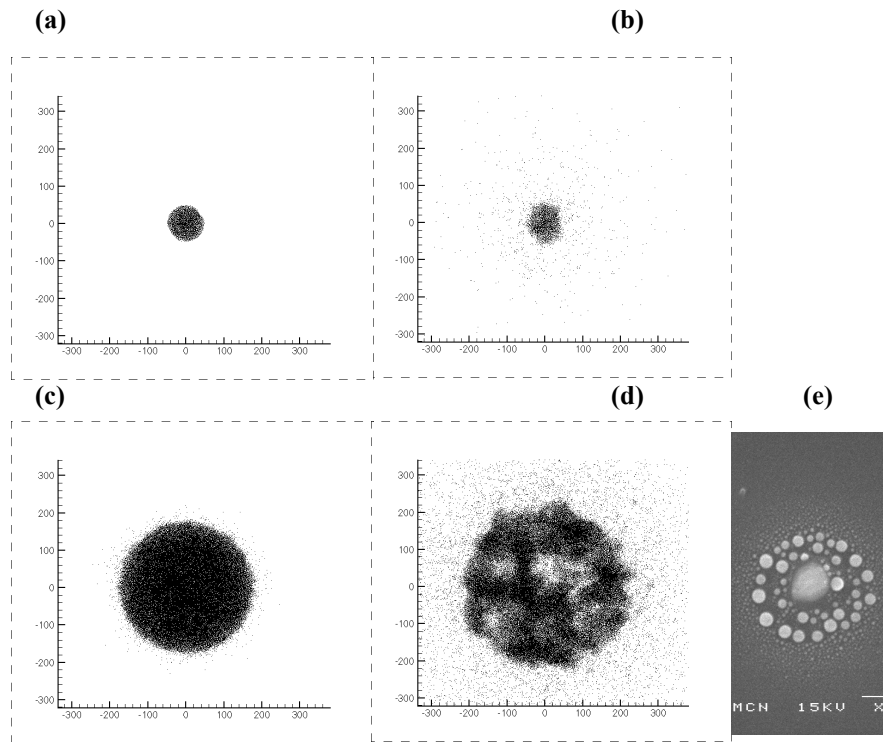


Figure 8.(a)-(b) Snapshots from MD simulations showing one small nanoparticle upon absorption of laser radiation; (c)-(d) –the same for larger nanoparticle. (e) MEB image of a gold particle on Si substrate after laser irradiation.

One of the commonly used methods of NP's size reduction and/or shape modification is additional laser irradiation. In fact, upon absorption of laser radiation, particles can melt, change their shape, evaporate or suffer a fragmentation due to both mechanical effects and/or Coulomb explosion. Our MD calculations (Figure 8) have clearly demonstrated that upon absorption of the same energy per monomer, smaller particles tend to evaporate, whereas larger ones are fragmented. Here, particles were composed of a molecular solid material and fragmentation was mechanical due to pressure wave propagation towards the center of the particle, its reflection and the following rarefaction wave formation. To observe such effects, the radius of particle should be high enough, simple thermal evaporation was observed. These results agree with recent experimental (Figure 8e and experimental results⁶⁶).

5. SUMMARY

To summarize, we have considered a number of mechanisms involved in NPs and nanostructure formation with the aid of laser pulses. In particular, rapid target fragmentation, nucleation, aggregation, particle diffusion and coalescence on substrate, their behavior in liquid solutions and upon additional laser irradiation have been considered. In particular, we have considered the question of NP's size distribution and its shape.

The performed analysis allows one to better understand what parameters can be used to control the NPs and nanostructure formation. The presented analysis can be, thus, helpful for the development of controlled nano-assembly methods for fabrication of nano- and meta-materials.

ACKNOWLEDGEMENTS

The authors are grateful to Dr. W. Marine, Prof. L. Zhigilei, Dr. Zh. Lin, and Dr. M. Povarnitsyn for the insightful suggestions and valuable advises. In addition, the super-computer center CINES of CNRS, France is acknowledged for computer support under the project c2011085015

REFERENCES

-
- [1] Marine, W., Patrone, L., Luk'yanchuk, B., Sentis, M., "Strategy of nanocluster and nanostructure synthesis by conventional pulsed laser ablation" *Appl. Surf. Sci.* 154-155, 345 (2000).
 - [2] Ozerov, I., Nelson, D., Bulgakov, A., Marine, W., Sentis, M. "Synthesis and laser processing of ZnO nanocrystalline thin films." *Appl. Surf. Sci.* 212-213, 349 (2003).
 - [3] Luk'yanchuk, B., Marine, W., and Anisimov, S., "Mechanisms of Nanoparticle Formation by Laser Ablation" *Laser Phys.* 8, 291 (1998).
 - [4] Luk'yanchuk, B. S., Marine, W., Anisimov, S. I., Simakina, G. A., "Condensation of vapor and nanoclusters formation within the vapor plume, produced by ns-laser ablation of Si, Ge and C" *Proc. of SPIE*, 3618, 434-452 (1999).
 - [5] Ohkubo, T., Kuwata, M., Luk'yanchuk, B., Yabe, T., "Numerical analysis of nanocluster formation within ns-laser ablation plume" *Appl. Phys. A* 77, 271 (2003).
 - [6] Itina, T. E., Tokarev, V. N., Marine, W., Autric, M., *J. Phys. Chem.* "Monte Carlo simulation study of the effects of nonequilibrium chemical reactions during pulsed laser desorption" 106, 8905 (1997).
 - [7] Itina, T. E., Patrone, L., Marine, W., Autric, M., "Numerical analysis of TOF measurements in pulsed laser ablation" *Appl. Phys. A* 69, s59 (1999).
 - [8] Breihl, B., Urbassek, H. M "Monte Carlo simulation of growth and decay processes in a cluster aggregation source" *J. Vac. Sci. Technol. A*, 17, 256 (1999).
 - [9] Zhigilei, L. V., Garrison, B. J., "Microscopic mechanisms of laser ablation of organic solids in the thermal and stress confinement irradiation regimes" *J. Appl. Phys.* 88, 1281 (2000).
 - [10] Itina, T. E., Zhigilei, L. V., Garrison, B. J., "Microscopic mechanisms of matrix assisted laser desorption of analyte molecules: insights from molecular dynamics simulation" *J. Phys. Chem. B* 106, 303-310 (2002).
 - [11] Zeifman, M. I., Garrison, B. J., Zhigilei, L. V., "Combined molecular dynamics - direct simulation Monte Carlo computational simulation of laser ablation plume evolution," *J. Appl. Phys.* 92, 2181 (2002).
 - [12] Tsui, Y. Y., Santiago, J., Li, Y. M., Fedosejevs, R., "Melting and damage of aluminum surfaces by 80 ps KrF laser pulses," *Opt. Commun.* 111, 360 (1994).
 - [13] Komashko, A. M., Feit, M. D., Rubenchik, A. M., Perry, M. D., Banks, P.S., "Metal Processing with Ultra-Short Laser Pulses," *Appl. Phys. A* 69, s95 (1999).
 - [14] Eidmann, K., Meyer-ter-Vehn, J., Schlegel T., Hüller, S., "Hydrodynamic simulation of subpicosecond laser interaction with solid-density matter," *Phys. Rev. E* 62(1), 1202 (2000).
 - [15] Anisimov, S. I., Bonch-Bruевич, A. M., El'yashevich, M. A., Imas, Ya. A., Pavlenko, N. A., Romanov, G. S., "The action of high-power light fluxes on metals," *Sov. Phys.-Tech. Phys.*, 11, 945 (1967).
 - [16] Anisimov, S. I., Luk'yanchuk, B. S., "Selected problems of the theory of laser ablation," *Uspehi Fiz. Nauk*, 172 (3), 301 (2002).
 - [17] Rethfeld, B., Sokolowski-Tinten, K., von der Linde, D., Anisimov, S. I., "Ultrafast thermal melting of laser-excited solids by homogeneous nucleation," *Phys. Rev. B* 65, 092103 (2002).
 - [18] Vidal, F., Johnston, T. W., Laville, S., Barthélemy, O., Chaker, M., Le Droff, B., Margot, J., Sabasi, M., "Critical-point phase separation in laser ablation of conductors," *Phys. Rev. Lett.*, 86, 2573 (2001).
 - [19] Bulgakova, N. M "Possibility of rarefaction shock wave under short pulse laser ablation of solids," *Phys. Rev. E*, 60, R3498 (1999).
 - [20] Gamaly, E., Rode, A., Luther-Davies, B., Tikhonchuk, V., "Ablation of solids by femtosecond lasers: Ablation mechanism and ablation thresholds for metals and dielectrics," *Phys. Plasm.*, 9 (3), 949 (2002).
 - [21] Zhigilei, L. V., Garrison, B. J., *Appl.* "Molecular dynamics simulation study of the fluence dependence of particle yield and plume composition in laser desorption and ablation of organic solids" *Phys. Lett.*, 74, 1341 (1999).

- [22] Garrison, B. J., Itina, T. E., Zhigilei, L. V., "Limit of overheating and the threshold behavior in laser ablation" *Phys. Rev. E.*, 68, 041501 (2003).
- [23] Du, D., Liu, X., Korn, G., Squier, J., Mourou, G., "Laser-induced breakdown by impact ionization in SiO₂ with pulse widths from 7 ns to 150 fs," *Appl. Phys. Lett.*, 64, 3071 (1994).
- [24] Lenzner, M., Krüger, J., Sartania, S., Cheng, Z., Spielmann, C., Mourou, G., Kautek, W., Krausz, F., "Femtosecond optical breakdown in dielectrics" *Phys. Rev. Lett.*, 80, 4076 (1998).
- [25] Stuart, B. C., Feit, M. D., Herman, S., Rubenchik, A. M., Shore, B. W., Pery, M. D. "Nanosecond-to-femtosecond laser-induced breakdown in dielectrics" *Phys. Rev. B.*, 53, 1749 (1996).
- [26] Mao, S. S., Quéré, F., Guizard, S., Mao, X., Russo, R. E., Petite, G., Martin, P., "Dynamics of femtosecond laser interactions with dielectrics" *Appl. Phys. A.*, 79, 1695 (2004).
- [27] Japara, J., Mero, M., Rudolph, W., Appl. "Retrieval of the dielectric function of thin films from femtosecond pump-probe experiments" *Phys. Lett.*, 80(15), 2637 (2002).
- [28] Jia, T. Q., Chen, H. X., Huang, M., Zhao, F. L., "Ultraviolet-infrared femtosecond laser-induced damage in fused silica and CaF₂ crystals" *Phys. Rev. B.*, 73, 054105 (2006).
- [29] Sanner, N., Utéza, O., Bussiere, B., Coustillier, G., Leray, A., Itina, T., Sentis, M., "Measurement of femtosecond laser-induced damage and ablation thresholds in dielectrics" *Appl. Phys. A.*, 94, 889 (2009).
- [30] Perez, D., Lewis, L. J., "Molecular-dynamics study of ablation of solids under femtosecond laser pulses" *Phys. Rev. B.*, 67, 184102 (2003)
- [31] Itina, T. E., Zhigilei, L. V., Garrison, B. J., "Microscopic mechanisms of matrix assisted laser desorption of analyte molecules: Insights from molecular dynamics simulation" *J. Phys. Chem. B*, 106, 303-310 (2002).
- [32] Itina, T. E., Zhigilei, L. V., Garrison, B. J., "Matrix-assisted pulsed laser evaporation of polymeric materials: a molecular dynamics study" *Nuclear Instr. & Methods in Phys. Res. B, Beam Interaction with Materials and Atoms.*, 180, 238-244 (2001).
- [33] Itina, T. E., Marine, W., Autric, M., "Monte Carlo simulation of pulsed laser ablation from two-component target into diluted ambient gas" *J. Appl. Phys.*, 82(7), 3536 (1997).
- [34] Itina, T. E., Hermann, J., Delaporte P., Sentis, M., "Laser-generated plasma plume expansion: Combined continuous-microscopic modeling" *Phys. Rev. E*, vol. 66, 066406 (2002).
- [35] Itina, T. E., Tokarev, V. N., Marine, W., Autric, M., "Monte Carlo simulation study of the effects of nonequilibrium chemical reactions during pulsed laser desorption" *J. Chem. Phys.*, 106(21), 8905 (1997).
- [36] Povarnitsyn, M. E., Itina, T. E., Sentis, M., Khishenko, K. V., Levashov, P. R., "Material decomposition mechanisms in femtosecond laser interactions with metals" *Phys. Rev. B.*, 75, 235414 (2007).
- [37] Povarnitsyn, M. E., Itina, T. E., Khishchenko, K. V., Levashov, P. R., "Suppression of ablation in femtosecond double-pulse experiments" *Phys. Rev. Lett.*, 103, 195002 (2009).
- [38] Song, K. H., Xu, X., Appl. "Explosive phase transformation in excimer laser ablation" *Surf. Sci.*, 127-129, 111-116 (1998).
- [39] Bennett, T. D., Grigoropoulos, C. P., Krajnovich, D. J., "Near - threshold laser sputtering of gold" *J. Appl. Phys.*, 77, 849-864 (1995).
- [40] Serna, R., Dreyfus, R. W., Solis, J., Afonso, C. N., Allwood, D. A., Dyer, P. E., Petford-Long A. K., "Matrix assisted laser desorption/ionisation studies of metallic nanoclusters produced by pulsed laser deposition" *Appl. Surf. Sci.*, 127-129, 383-387 (1998).
- [41] Yoo, J. H., Jeong, S. H., Mao, X. L., Greif, R., Russo, R. E., "Evidence for phase-explosion and generation of large particles during high power nanosecond laser ablation of silicon" *Appl. Phys. Lett.*, 76, 783-785 (2000).
- [42] Yoo, J. H., Jeong, S. H., Greif, R., Russo, R. E., "Explosive change in crater properties during high power nanosecond laser ablation of silicon" *J. Appl. Phys.*, 88, 1638-1649 (2000).
- [43] Okano, A., Takayanagi, K., "Neutral silicon clusters produced by laser ablation in vacuum" *Appl. Surf. Sci.*, 127-129, 362-367 (1998).
- [44] Marine, W., Patrone, L., Luk'yanchuk, B., Sentis, M., "Strategy of nanocluster and nanostructure synthesis by conventional pulsed laser ablation" *Appl. Surf. Sci.*, 154-155, 345-352 (2000).
- [45] Webb, R. L., Dickinson, J. T., Exarhos, G. J., "Characterization of Particulates Accompanying Laser Ablation of NaNO₃" *Appl. Spectrosc.*, 51, 707-717 (1997).
- [46] Kozlov, B. N., Mamyrin, B. A., "Mass spectrometric analysis of clusters formed in laser ablation of a sample" *Tech. Phys.*, 44, 1073-1076 (1999).
- [47] Hankin, S. M., John, P., *J. Phys. Chem. B.*, "Microstructural Studies of CVD Diamond Films by Transmission Electron Microscopy" 103, 4566-4569 (1999).
- [48] Callies, G., Schittenhelm, H., Berger, P., Hügel, H., "Measurements of wavelength-dependent transmission in excimer laser-induced plasma plumes and their interpretation" *Appl. Surf. Sci.*, 127-129, 134-141 (1998).
- [49] Mizuseki, H., Jin, Y., Kawazoe, Y., Wille, L. T., "Growth Processes of Magnetic Clusters Studied by Direct Simulation Monte Carlo Method" *Appl. Phys. A.*, 73, 731 (2001).
- [50] Hermann, J., Noël, S., Itina, T. E., Appl. "Nanoparticle generation in plasmas produced by ultra-short laser pulses" *Surf. Sci.*, 253 (15), 6310-6315 (2007).

-
- [51] Hermann, J., Noël, S., Itina, T. E., Axente, T. E., Povarnitsyn, M. E., “Correlation between ablation efficiency and nanoparticle generation during the short-pulse laser ablation” *Laser Physics* 18(4), 374 (2008).
- [52] Amoroso, S., Ausanio, G., Barone, A.C., Bruzzese, R. Campana, C., Wang, X., “Nanoparticles size modifications during femtosecond laser ablation of nickel in vacuum”, *Appl. Surf. Sci.* 254, 1012–1016 (2007).
- [53] Eliezer, S. et al. “Synthesis of nanoparticles with femtosecond laser pulses”, *Phys. Rev B* 69, 144119 (2004).
- [54] Dubowski, J. J. [Photon-based nanoscience & nanobiotechnology], NATO Science series II: Mathematics, physics & chemistry, 239 (2007)
- [55] Volmer, M., and Weber, A *Z. Phys. Chem. (Leipzig)* 119, 277 (1926).
- [56] Becker, R. and Döring, W., *Ann. Phys.* 5, 719 (1935).
- [57] Reiss, H. “The Kinetics of Phase Transitions in Binary Systems,” *J. Chem. Phys.* 18, 840 (1950).
- [58] Kashchiev, D., [Nucleation, Basic Theory with Applications], Butterworth-Heinemann, Oxford, 2000.
- [59] Anisimov S. I. et al, [High power laser action on metals], Nauka, Moscow, 1970.
- [60] Gusarov, A., Gnedovets, G., Smurov, I., and Flamant, G. “Simulation of nanoscale particles elaboration in laser-produced erosive flow” *Appl. Surf. Sci.*, 154–155, 331 (2000).
- [61] Holian, B.L., Grady, D. “Fragmentation by molecular dynamics: The microscopic “big bang”” *Phys. Rev. Lett.* 60,1355 (1988).
- [62] Ashurst, W.T., Holian, “Droplet formation by rapid expansion of a liquid” B.L., *Phys. Rev. E* 59, 6742 (1999).
- [63] P. Peeters, *Nucleation and Condensation in Gas-Vapor Mixtures of Alkanes and Water*, Eindhoven : Technische Universiteit Eindhoven, 2002.
- [64] Dekker, P. and Friedlander, Sh. K., “The Self-Preserving Size Distribution Theory:: I. Effects of the Knudsen Number on Aerosol Agglomerate Growth” *J. of Colloid and Interface Science*, 248, 2,295-305 (2002).
- [65] Robb, D. T., Halaciuga, I., Privman, V., Goia, D. V., “Computational model for the formation of uniform silver spheres by aggregation of nanosize precursors” *J. Chem. Phys.* 129, 184705 (2008).
- [66] Pyatenko, A., Yamaguchi, M., Suzuki, M., “Mechanisms of size reduction of colloidal silver and gold nanoparticles irradiated by Nd: YAG Laser” *J. Phys. Chem. C*, 113, 9078–9085 (2009).